Nuclear Physics **A363** (1981) 9–34

NEUTRON PARTICLE-HOLE ELECTRIC DIPOLE STATES IN ^{206,207,208}Pb†

P.A. DICKEY

University of Washington, Seattle, WA 98195, *USA*

Received 10 September 1980

Abstract: Inelastic proton scattering on ^{206}Pb, ^{207}Pb and ^{208}Pb through isobaric analog resonances has been used to study neutron particle-hole excitations with large ground-state γ-branches in these Pb isotopes. Relative (p, p') cross sections at 90° are extracted for structures selectively excited on the $d_{5/2}$, $s_{1/2}$, and $d_{3/2}-g_{7/2}$ resonances. Interpretation of excitations is ^{206}Pb and ^{207}Pb in terms of coupling to states in ^{208}Pb is discussed. Branching ratios for 1^- states in ^{208}Pb at 4.84, 5.29, 5.94 and 6.31 MeV and the $\frac{1}{2}^+$ state in ^{207}Pb at 4.63 MeV are deduced.

E NUCLEAR REACTIONS ^{206,207,208}Pb(p, p'γ); $E = 16.2$–17.8 MeV; measured E_p, I_p, pγ-coin; deduced $\sigma(\theta)$. ^{207,208}Pb levels deduced Γ_γ/Γ. Enriched targets.

1. Introduction and summary of previous results

Recent experiments [1]) have revealed striking similarities in the energy dependence of the photon elastic scattering cross section below neutron threshold in ^{206}Pb, ^{207}Pb, ^{209}Bi and doubly magic ^{208}Pb (see fig. 1). These similarities in dipole transition strength suggest a relatively weak coupling of valence particles (or holes) to $J^\pi = 1^-$ excitations of the ^{208}Pb core. The weak coupling model [2]) has been highly successful in describing the septuplet of levels near 2.6 MeV in ^{209}Bi formed by coupling the valence proton to the 3^- collective octupole state in ^{208}Pb [3–5])]. The model has also been proposed for a number of higher-lying levels in neighboring nuclei including some electric dipole states in ^{207}Pb up to 7 MeV in excitation [6–8]). On the other hand, a detailed study of low-lying 2p-1h levels in ^{209}Bi has shown that the coupling of the valence proton to the non-collective 4^- and 5^- neutron p-h states of ^{208}Pb is not strictly weak [9]). It is important to learn how high in excitation energy weak coupling occurs and for what types of core excitations it applies.

We have studied the p-h structure of some dipole states in ^{206}Pb, ^{207}Pb and ^{208}Pb, excited through the (p, p'γ_0) reaction on isobaric analog resonances (IAR). In ^{206}Pb and ^{207}Pb we observe probable examples of both the weak and the strong coupling of neutron holes to ^{208}Pb dipole core states up to about 6 MeV in excitation energy. Our results are consistent with what is already known experimentally [10–12]) about the shell-model structure of the ^{208}Pb core states. As a by-product of this experiment we

† Research supported by the US Energy Research and Development Administration.

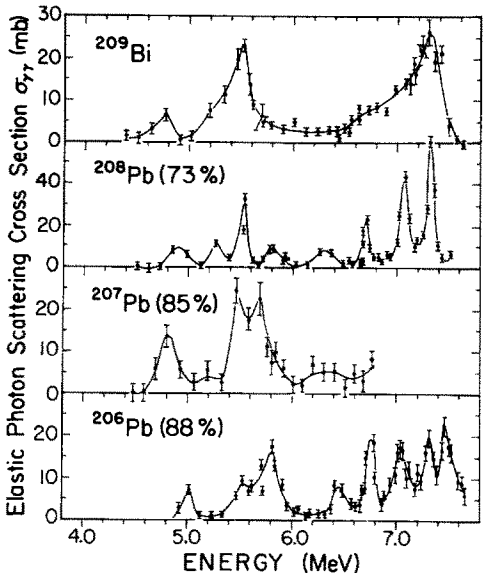

Fig. 1.Comparison of (γ,γ) cross sections as a function of energy for nuclei near ^{208}Pb. Data is from Laszewski and Axel [1]). Energy resolution is comparable to the point spacing.

have obtained the ground-state γ-ray branching ratios Γ_{γ_0}/Γ of the 4.84, 5.29, 5.94 and 6.31 MeV, $J^\pi = 1^-$ states in ^{208}Pb and the 4.63 MeV, $\frac{1}{2}^+$ state in ^{207}Pb. These branching ratios are needed in order to extract the γ-ray widths of the levels from resonance fluorescence measurements of $(\Gamma_{\gamma_0})^2/\Gamma$. The deviations from 100% which we find for some of these branching ratios will not significantly affect the deduced dipole strength of the levels, but they may be clues to the microscopic structure of the levels.

The low-lying discrete 1^- states in ^{208}Pb have been studied primarily with the (γ, γ [refs. [1,6–8,13,14])], (p, p') [ref. [12])], (e, e') [ref. [15])] and (d, p) [refs. [10,11,16])] reactions. It is known from nuclear resonance fluorescence [6]) and elastic photon scattering [1]) that about 1.5% of the total El strength in ^{208}Pb is found in two so-called "mini-resonances" centered at about 5.5 and 7.2 MeV excitation. Shell-model calculations [17,18]) predict that the 1^- states near 5.5. MeV include mainly mixtures of neutron p-h configurations while those around 7.2 MeV are predominantly proton p-h states. This partition is ascribed to the difference in mean energies of neutron p-h and proton p-h excitations in the unperturbed shell model. Harvey and Khanna [18]) have noted further that the 5.5 and 7 MeV "mini-resonances," which are generally reproduced in their calculation, are truly "collective" in the sense that no one p-h configuration appears with intensity greater than 15%. Conversely, eigenstates which have large configuration intensities carry little dipole strength. They also find that the spreading in energy of a configuration over the eigenstates increases with the spins of the particle and hole involved; thus $s_{1/2}p_{1/2}^{-1}$ would be the most localized

TABLE 1

Properties of bound 1^- levels in ^{208}Pb

Excitation (MeV)	Γ_0(eV) ref. [6])	$\frac{1}{3}(2J+1)S$(d, p) ref. [10])	$\frac{1}{3}(2J+1)S$(d, p) ref. [11])	Configuration
4.84	6.3			mixed neutron p-h
5.29	8.6	0.90 [a])	1.17 [a])	$s_{1/2}p_{1/2}^{-1}$
5.51	28		0.05	mixed neutron p-h
5.63 [b])				
5.94		0.47	0.73	$d_{3/2}p_{1/2}^{-1}$
6.26 [c])	4.1			
6.31 [c])	1.0			$s_{1/2}p_{3/2}^{-1}$
6.49				
6.72	15			
7.06	29			
7.08	14			$d_{3/2}$ or $g_{7/2}$
7.33	38			

[a]) $\frac{1}{4}(2J+1)S_{d,p}$. Value of $\frac{1}{3}(2J+1)S_{d,p} > 1$ indicates 0^- and 1^- levels as doublet.
[b]) Level seen in ref. [12]). Not positively identified as 1^-.
[c]) Parity assignment is probable, but not certain.

configuration. These general features are confirmed by spectroscopic factors from ^{207}Pb(d, p) [refs. [10,11])] and ^{208}Pb(p, p') [refs. [12,19])] experiments.

In table 1 we have listed some properties of the known [20]) spin-1 bound states in ^{208}Pb: their radiative widths [6]), (d, p) spectroscopic factors [10,11]), and principal p-h configurations [19]). The results of previous experiments have been summarized by Coope *et al.* [6]); we reiterate them here with some additions:

(i) Only two 1^- states are strongly populated in ^{207}Pb (d, p) and thus have significant admixtures of $p_{1/2}^{-1}$ neutron configurations. The 5.29 MeV state nearly exhausts the $s_{1/2}p_{1/2}^{-1}$ configuration strength not included in the giant dipole resonance. The 5.94 MeV state comprises most of the $d_{3/2}p_{1/2}^{-1}$ configuration strength; it is not seen in (γ, γ) experiments. The remaining $d_{3/2}$ strength is apparently fragmented among many levels.

(ii) The 6.31 MeV state exhausts a major fraction of the $s_{1/2}p_{3/2}^{-1}$ strength [12]).

(iii) The structure of the 4.84 MeV state has been described as "collective" [19]), i.e., having a mixed neutron p-h structure. Swann [21]) reported an M1 excitation at this energy; a claim doubted by DelVecchio *et al.* [22]), who established a 1^- assignment for the level at 4.841 ± 0.005 MeV. In light of this and a new measurement of his own, Swann [23]) has proposed a doublet of 1^+ and 1^- levels within 3 keV.

(iv) The 5.51 MeV state has a mixed neutron p-h structure and is strongly excited in (γ, γ) reactions.

(v) The 7 MeV levels (7.06, 7.08, and 7.33 MeV) comprise over half of the total radiative width below threshold. The 7.06 MeV level was proposed as an M1 excitation [24]), but more recent experiments [25,26]) show that all three levels are 1^-.

(vi) The states most strongly excited in photon scattering appear to have mixed configurations [6]).

In contrast to ^{208}Pb almost nothing is known about the low-lying dipole states of ^{206}Pb and ^{207}Pb because the level density in these nuclei is much greater than it is at the same excitation energy in ^{208}Pb. Photon scattering data [1]) show an indication of weak coupling states without resolving individual levels in ^{206}Pb and ^{207}Pb. The (p, p'γ) reaction through analog resonances tests the weak coupling model by probing the p-h structure of the levels excited in (γ, γ) reactions, allowing one to trace their parentage to the 1^- core states in ^{208}Pb.

2. Inelastic proton scattering through IAR

Isobaric analog resonance inelastic proton scattering selectively populates neutron p-h states in closed shell nuclei [19]). The process is illustrated in fig. 2 for the case of a ^{208}Pb target. The wave function of the analog state ψ_A is obtained from that of its parent ψ_{PA} by the application of the isospin lowering operator T^-:

$$\psi_A(J, T-1) = \frac{1}{(2T)^{1/2}} T^- \psi_{PA}(J, T) = \frac{1}{(2T)^{1/2}} \sum_j (t_j^-) \psi_{PA}(J, T) . \qquad (1)$$

In this expression (J, T) represents the spin and z-component of isospin of the parent state, and t_j^- is the isospin lowering operator which acts on the particle j (j denotes the spin of the particle). If the single-neutron parent state in ^{209}Pb is written as a product of a single-neutron wave function $\phi_n(J)$ and the ^{208}Pb ground state core $\phi_c(0^+)$,

$$\psi_{PA}(J, T) = \phi\text{-}(J)\phi_c(0^+) , \qquad (2)$$

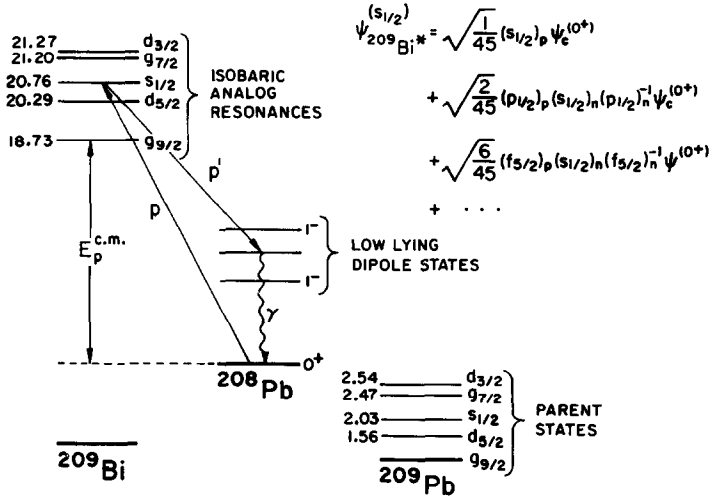

Fig. 2. Schematic illustration of the ^{208}Pb(p, p'γ) reaction on isobaric analog resonances in ^{209}Bi. The first three terms of the $s_{1/2}$ analog state wave function are shown.

one finds that the analog state is a superposition of a single-proton state and many 2p-1h states:

$$\psi_A(J, T-1) = \frac{1}{(2T)^{1/2}} \left(\phi_p(J)\phi_c(0^+) + \phi_n(J) \sum_j [\phi_p(j)\phi_n^{-1}(j)]_{0^+}\phi_c(0^+) \right). \quad (3)$$

The analog resonance is excited through the first term in eq. (3) and decays by emission of a proton $\phi_p(j)$ from one of the 2p-1h configurations indicated in the summation, leaving the target in the neutron p-h state $\phi_n(J)\phi_n^{-}(j)$. The spin J of the neutron particle is the same as that of the incident proton and of the IAR; similarly the spin j of the hole and the outgoing proton are identical. Because the particle and hole are in different oscillator shells, negative-parity states are usually formed. Fig. 3 shows the available neutron orbitals for $N = 126$.

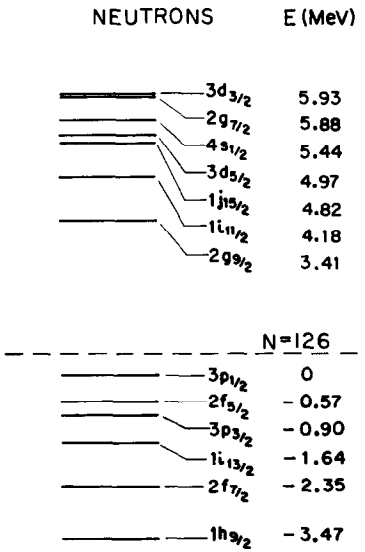

Fig. 3. Neutron orbitals in the vicinity of the $N = 126$ shell closing. The energies are taken from ref. [19]).

The strong ground-state γ-ray decay of electric dipole, neutron p-h states in heavy nuclei [12]) identifies these states in the (p, p'γ_0) reaction even when the total level density is high. Although M1 and E2 states also have large γ_0 branches, positive-parity states in ^{208}Pb are not expected to show resonant behavior on the $g_{9/2}$, $d_{5/2}$, $s_{1/2}$, $d_{3/2}$, or $g_{7/2}$ IAR.

Total resonance (p, p') cross sections are related to the parentage coefficients a^I_{Jj} for neutron p-h configurations by the equation

$$\sigma^I = \frac{2I+1}{2} \pi\lambda \frac{2\Gamma_p^J/\Gamma^J}{\Gamma^J} \sum_j |a^I_{Jj}|^2 \Gamma_j^{SP}, \quad (4)$$

in which I is the spin of the state populated in (p, p'), (J, j) is the spin of the neutron

(particle, hole), Γ^J is the proton partial width of the single neutron IAR, Γ^J is the total width of the IAR and Γ_j^{SP} is the single-particle width for emission of a proton of spin j. The sum over neutron holes implies that the resonance behavior of the total (p, p') cross section can identify only the particles in the p-h configurations. Fortunately the holes which can couple with a given particle spin J to form $I = 1$ are limited to those with $j = J, J \pm 1$ for $J > \frac{1}{2}$ and $j = J, J+1$ for $J = \frac{1}{2}$, and the factor Γ_j^{SP} is largest for holes with the lowest relative orbital momentum. One or two terms dominate the sum over j in most instances. Real selectivity in populating p-h configurations is obtained with the (d, p) reaction, but only the hole states already in the target ($p_{1/2}^{-1}$ for ^{207}Pb) can be reached. Together, (d, p) and (p, p') data provide reasonably quantitative intensities for the major neutron p-h configurations in the 1^- states of ^{208}Pb.

The foregoing discussion carries over to the case of ^{206}Pb(p, p'γ), only here the $p_{1/2}$ neutron shell is empty. A more complicated situation arises for the ^{207}Pb target unless weak coupling applies. In that event the cross section (total or differential) for populating the weak coupling doublet in ^{207}Pb would have the same energy dependence as that of the core state in ^{208}Pb. A beautiful example is the 2.6 MeV septuplet in ^{209}Bi studied by Coffin *et al.* [5]).

3. The experiment

We have used the IAR (p, p'γ) reaction to study clusters of dipole states in ^{206}Pb and ^{207}Pb to see if they are selectively excited on resonance as are the discrete 1^- states in ^{208}Pb. The strong ground-state γ-ray decay of dipole states can select these states, or at least groups of these states, from the dense background of higher spin levels excited in nuclear reactions. Our energy resolution of 35 keV is to be compared to about 100 keV for the photon scattering data of Laszewski and Axel [1]).

The proton beam from the University of Washington FN tandem accelerator bombarded targets of enriched ^{206}Pb, ^{207}Pb and ^{208}Pb. Typically 50 to 200 nA of beam current was incident upon the 0.5-1 mg/cm^2 self-supporting lead foils. The experimental setup is shown in fig. 4. Protons were detected at 90° in a Si(Li) detector 3 mm thick, collimated with a 0.64 cm × 1.59 cm aperture 7.94 cm from the target. The detector was cooled in the chamber with a thermoelectric junction and was equipped with an electron sweeping magnet. Fig. 5 shows a proton spectrum with 34 keV energy resolution, the best attained with this system. An anticoincidence shielded 25.4 cm × 25.4 cm NaI crystal, collimated to an acceptance angle of ± 7.5°, was the γ-ray detector. Coincidences between protons and γ-rays were recorded with the NaI crystal at several angles between 45° and 135° in the reaction plane; an out-of-plane measurement was made for the ^{207}Pb and ^{208}Pb targets by rotating the scattering chamber 90° azimuthally around the beam axis. Spectra were collected at energies corresponding to the $s_{1/2}$, $d_{5/2}$ and $d_{3/2} - g_{7/2}$ resonances and off resonance for all the targets.

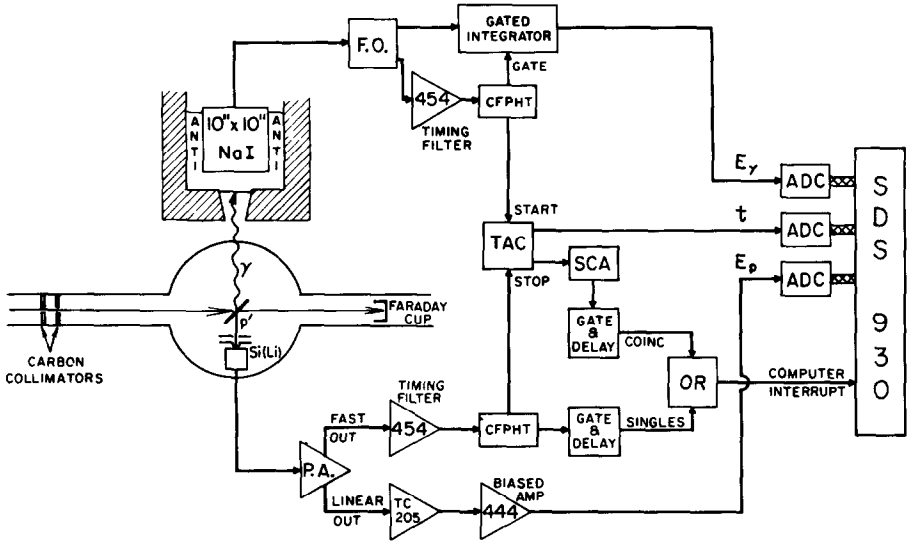

Fig. 4. Schematic diagram of the experimental arrangement showing a simplified version of the electronics.

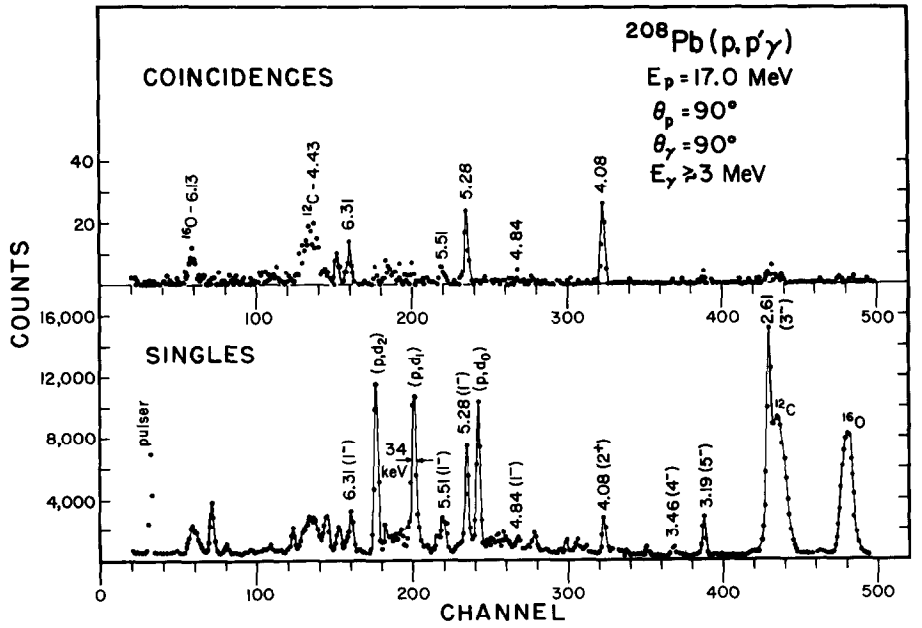

Fig. 5. Singles and coincidence particle spectra for a typical run with the ^{208}Pb target. The indicated energy resolution of 34 keV was the best attained with the Si(Li) detector.

Three parameter (E_p, E_γ and TAC) coincidence data were written event-by-event on magnetic tape. The proton singles and coincidence signals were handled simultaneously by one ADC. On playback of the data tapes, a software window was placed around the prompt coincidence peak in the TAC spectrum. Two-dimensional proton energy versus γ-ray energy spectra were generated for events in the TAC window, and a sum along the kinetic locus for (p, p'γ_0) was projected onto an axis representing excitation energy in the final nucleus.

The geometry chosen for the experiment was a compromise. The undesirable (for our purposes) coherence of the direct-compound interference is reduced if one does not observe the scattered protons in a (p, p'γ) reaction, as was the case in the ^{208}Pb(p, p'γ) study of Cramer *et al.* [12]). In our experiment, however, the proton detector was required for energy resolution because the high neutron flux dictated the use of a NaI detector for the γ-rays. An advantage of a coincidence experiment is that quite precise γ-ray branching ratios can be measured if a clean proton singles spectrum can be obtained. Our particle detector energy resolution was only comparable to the average level spacing in ^{208}Pb between 4 and 7 MeV, so we chose to place the detector at $\theta_p = 90°$ because for this angle (p, p') data with a 9 keV energy resolution exist in the literature [19]).

Runs at several γ-ray detector angles were added together to average over the proton-γ angular correlation. It is demonstrated in the appendix that for $J = 1 \rightarrow 0$ γ-ray transitions the total γ-ray yield can be obtained exactly from one out of plane and two in plane measurements, the latter separated in angle by 90°. The same can be shown to be true for the dipole γ-ray transitions in ^{207}Pb. For the ^{208}Pb target, this procedure was followed, and the (p, p'γ_0) coincidence yields we report are proportional to $(d\sigma/d\Omega)(p, p')|_{90°}$. The total γ-ray yields from the states in ^{208}Pb were used to determine ground-state branching ratios. For the ^{206}Pb the p-γ correlation was only approximately averaged by adding data taken at five angles between 55° and 125° in the reaction plane. Some ^{207}Pb data was taken in each of the two γ-ray geometries.

The proton singles spectra could not be used to obtain branching ratios for the 1^- states in ^{208}Pb because frequently in the vicinity of a $J = 1$ state several known levels fell within the 34 keV detector resolution, and a sufficiently accurate background subtraction was impossible. Therefore, the relative differential cross sections at 90° were taken from the 9 keV spectrograph data of Moore *et al.* [19]). Even in higher resolution data [27]) there are indications of unresolved multiplets, precluding the branching ratio determination for some of the levels. Absolute normalization to our coincidence yields was made with the 5.29 MeV state in the simultaneous proton singles spectrum, shown in fig. 6, because this state had the largest cross section and the singles spectrum seemed relatively clean. The background was determined by fitting the proton peak in singles with a lineshape derived channel by channel from the coincidence spectrum.

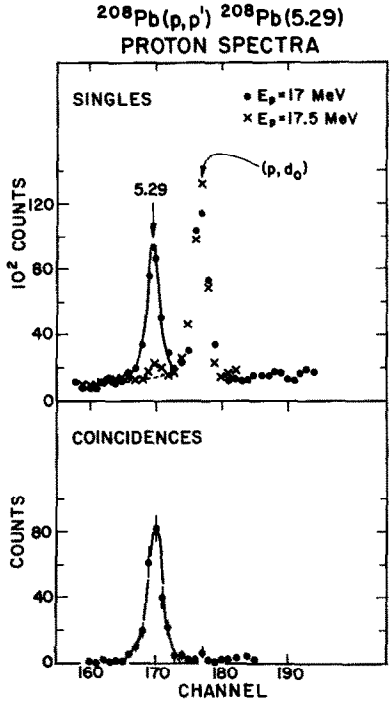

Fig. 6. A portion of the singles and coincidence particle spectra showing the 5.29 MeV, 1^- state in ^{208}Pb which is enhanced at $E_p = 17$ MeV. Least-squares fit (solid curve) to this peak in singles was used to normalize the present coincidence data to the proton singles data of ref. [19]). A spectrum obtained off the $s_{1/2}$ resonance at $E_p = 17.5$ MeV (crosses) is consistent with the background determined from the fit.

The absolute efficiency of the NaI detector at 4.43 MeV is known from a previous coincidence measurement [28]). Extrapolation to 7 MeV was made using the known weak energy dependence of the gamma ray absorption for the material in front of the crystal. The absolute efficiency is accurate to within ± 5%

4. Results and discussion

4.1. ^{208}Pb

The (p, p'γ_0) reaction has been used previously to study 1^- neutron p-h states in ^{208}Pb [ref. [12])]. Our purpose in repeating some of that work was threefold. Since we were constrained to measure differential rather than total proton cross sections, it was necessary to perform ^{208}Pb measurements in the geometry to be used later for the other targets, the effects of the proton angular distribution being unknown. The second goal was to measure ground-state γ-ray branching ratios with 10% accuracy.

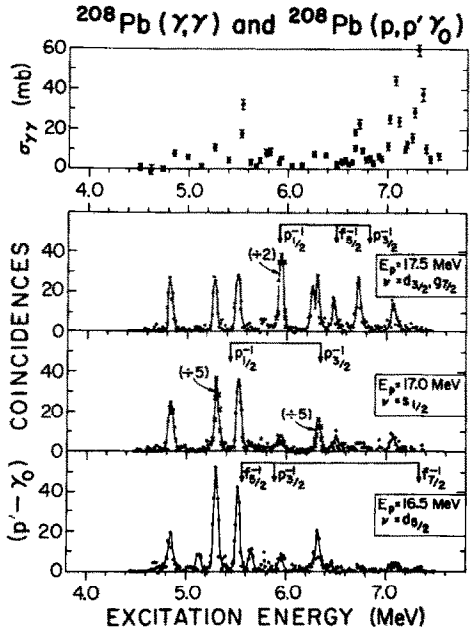

Fig. 7. Elastic photon scattering cross section [1]) and (p, p'γ_0) coincidence spectra (present work) for ^{208}Pb at the bombarding energies of the $d_{3/2}-g_{7/2}$, $s_{1/2}$, and $d_{5/2}$ analog resonances. Locus for $p'-\gamma_0$ coincidences events is $E_\gamma = E_{\gamma_0}{}^{+1\text{MeV}}_{-2\text{MeV}}$, random coincidences have been subtracted. Coincidence spectra for each target represent the same integrated beam current. Arrows indicate energies of unperturbed shell-model neutron p-h configurations which can couple to $J^\pi = 1^-$. Solid lines are merely to guide the eye.

A number of the branches deduced by Cramer *et al.* [12]) were significantly less than 100%, in apparent disagreement with Earl *et al.* [16]) but both of these experiments had accuracies of only 20–40%. Finally, in light of recent interest [24–26]) in the parity of the members of the 7.06–7.08 MeV $J = 1$ doublet, we hoped to see if the resonance yields of the two levels of the IAR were similar to each other and if they could rule out a positive parity assignment for either level. A 1^+ state would not be expected to show enhancements on any of the IAR studied here because the spin-orbit partners of the particle states are not available (see fig. 3).

Spectra of protons in coincidence with γ-rays to the ground state of ^{208}Pb are shown in fig. 7 and compared with $\sigma_{\gamma\gamma}$ from the work of Laszewski and Axel [1]). Selective excitation of the 1^- states on the IAR is readily apparent. Relative cross sections were deduced by summing the proton counts in each peak in coincidence with γ-rays in a window from 0.8 to 1.1 times the photopeak channel.

Table 2 compares our relative differential cross sections with the relative total cross sections from Cramer *et al.* [12]). The cross section for the 5.29 MeV state was normalized to 100 units in each case. It is clear that the differential and total cross

TABLE 2
Relative cross sections of states in ^{208}Pb on the IAR

Energy (MeV)	$d_{5/2}$		$s_{1/2}$		$d_{3/2}$	
	$\frac{d\sigma}{d\Omega_{90°}}$ this work	σ ref. [12])	$\frac{d\sigma}{d\Omega_{90°}}$ this work	σ ref. [12])	$\frac{d\sigma}{d\Omega_{90°}}$ this work	σ ref. [12])
4.84	14±1		16±1		17±1	
5.29	34±2	26	100 [a])	100 [a])	17±1	27
5.51	25±2	46	23±2	57	19±2	33
5.63	11±1	15				
5.94	9±1	10	9±1		44±2	50
6.26/6.31	14±1	26	49±2	58	21±1	26
6.49	7±1	7	11±1	7	15±1	11
6.73	3±1		6±1		30±1	11
7.07/7.09	6±1	11	9±1	9	12±1	12

[a]) All cross sections normalized to this value.

sections can differ from each other by as much as a factor of two, but the qualitative dependence on the entrance channel IAR is the same for both data sets. Thus, although it is not possible to extract quantitative spectroscopic factors from the differential cross sections using eq. (4), one can infer common parentage in states which exhibit similar analog resonance enhancement.

The branching ratios are given in table 3. We have used only relative (p, p') cross sections at 90° from Moore *et al.* [19]), normalized to our observed yield of the 5.29 MeV state in singles, thus freeing our results from systematic errors associated with uncertainties in target thickness, beam current integration, dead time corrections, and proton detector efficiency. Moreover, angular correlation effects have been completely taken into account. The limiting source of error in our deduced branches is the uncertainty in the cross sections of Moore *et al.* [19]) due to possible unresolved levels. In quoting errors on the branching ratios we have included all uncertainties except this crucial one; however, we have indicated in the footnotes to table 3 those energies at which multiplet structure was suspected in a 5–8 keV resolution (p, p') study at 35 MeV [ref. [27])].

Our results are in substantial agreement with the branching ratios reported by Cramer *et al.* [12]). Four of the states (4.84, 5.29, 5.94 and 6.31 MeV) clearly have ground-state branches in excess of 75%. Most γ-rays of energy 2.6 or 4.1 MeV in the coincidence spectra could be attributed to the decay of nearby known levels, but small (5–10%) branches feeding the 3^- or 2^+ states, for example, cannot be ruled out. The smaller apparent ground-state branches for the 5.51, 5.63 and 6.25 MeV states can only be considered lower limits because of the high probability of unresolved

TABLE 3

Ground-state branching ratios of levels in ^{208}Pb

Nucleus	E(MeV)	Γ_{γ_0}/Γ(%)			
		ref. [12])	present	ref. [14])	Footnotes
^{208}Pb	4.84		93±7	100	a)
	5.29	80±8	80±8	100	b)
	5.51	78±7	≥67±6	100	c)
	5.63	45±20	≥49±5		c)
	5.94	60±2	78±7	100	
	6.26	45±5	≥59±7	100	c)
	6.31	73±12	85±8	100	
	7.06	50±4			d)
	7.08				
^{207}Pb	4.63	$(\Gamma_{\gamma_0}/\Gamma = 0.86 \pm 0.09, \Gamma_{\gamma_1}/\Gamma \leq 0.03 \pm 0.06)$ $\Gamma_{\gamma_2}/\Gamma = 0.11 \pm 0.04$			

a) 4.1 MeV γ-rays in coincidence spectrum. On the basis of proton energy these $2^+ \rightarrow 0^+$ decays are probably fed from a state at 4.86 MeV reported in ref. [27]) to have a probable multiplet structure. We cannot absolutely rule out a 10% branch from the 4.84 to the 4.08 MeV state.

b) 4.1 MeV γ-rays in coincidence spectrum, perhaps from state at 5.27 MeV reported in ref. [27]), but we cannot rule out a 5% branch to the 4.08 MeV state. A 0^- state found in ref. [16]) to be only 8 keV lower in excitation than the 1^- state and excited in the (d, p) reaction could be included in the (p, p') cross section for the 5.29 MeV state. If so, with the $(2I+1)$ weighting the g.s. branch for the 5.29 MeV state becomes 107±9%.

c) High resolution (p, p') data of ref. [27]) indicate probable multiplet structure. Therefore g.s. branch given is only a lower limit.

d) 7.07–7.09 MeV doublet not resolved. See text.

levels in the singles proton spectra of ref. [16]). In each of these cases the higher resolution (p, p') study by Wagner *et al.* [27]) revealed a probable multiplet structure.

The 7.06–7.08 MeV doublet has received considerable attention recently as a result of evidence [24]) that the 7.06 MeV state might have positive parity and thus contain a significant fraction of the M1 strength in ^{208}Pb. Nathan *et al.* [26]), using polarized photon scattering, have now shown that both levels are indeed 1^-. There is great interest in the nuclear structure of these levels because they are strongly photoexcited [6]). Attempts to measure the ground-state branching ratios of these states [6,8,12,16,19]) have yielded inconsistent results, leaving the radiative widths of the states uncertain within a factor of two. Doublets reported at this energy in (p, p') experiments [19,27]) cannot be positively identified as the levels observed in (γ, γ) reactions.

We used a Si surface barrier detector in coincidence with the NaI spectrometer to observe the levels with 28 keV resolution at proton bombarding energies of 17.0, 17.25 and 17.5 MeV. The proton and γ-ray detectors were placed at 90° on either side of the beam to maximize the counting rate. The γ-ray coincidence guarantees

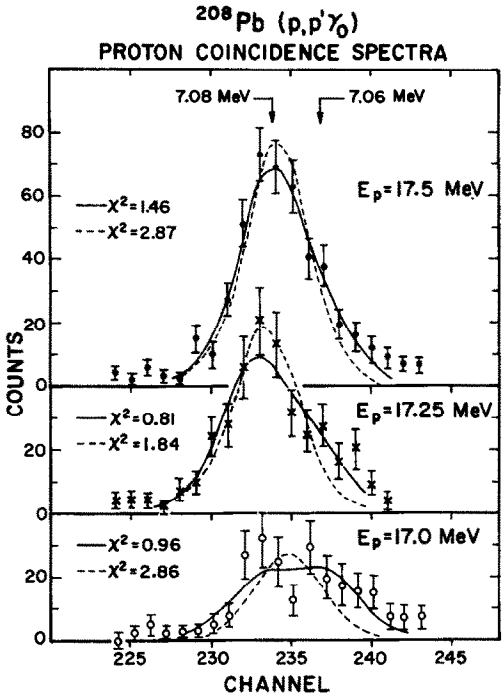

Fig. 8. Spectra of protons near the 7 MeV doublet in coincidence with ground-state γ-rays. Runs at three bombarding energies have been normalized to the same integrated beam current. Solid line is a least-squares fit with the peak energies constrained and using a line shape taken from the 3.198 MeV state in the proton singles spectrum, which is accumulated simultaneously with the same detector, electronics, and ADC as the coincidence spectrum. Dashed curve is a least-squares fit with a single peak whose energy was allowed to vary.

that levels we observe are those seen in (γ, γ). Our spectra are shown in fig. 8. Although the doublet was not completely resolved, fits of the spectra with experimental lineshapes from other proton peaks in the same runs clearly indicate that a doublet is present at all energies. The higher energy state at 7.08 MeV shows quite strong enhancement on the $d_{3/2}$, $g_{7/2}$ IAR, while the lower energy state has essentially the same cross section at all three energies. The resonance at 17.5 MeV would be expected for a 1^- state with some $d_{3/2}$ or $g_{7/2}$ neutron amplitude, but this behavior is not likely for a 1^+ state because the spin-orbit partners of the $d_{3/2}$ and $g_{7/2}$ neutron orbitals, which are above the Fermi level in ^{208}Pb, cannot participate as holes to form a positive-parity excitation. The energy dependence we observe is thus consistent with negative-parity assignments for both levels, but would not have ruled out a positive-parity assignment for the lower energy level. It does, however, point to a marked difference in nuclear structure between the two levels which have been suggested [6]) to be possibly dominated by proton 1p-1h configurations. Our results indicate a significant $d_{3/2}$ or $g_{7/2}$ neutron component in the 7.08 MeV level but not in

the 7.06 MeV level. They also raise the possibility that the 7.051 MeV state reported in (p, p') by Moore *et al.* [19]) is not the state strongly populated in (γ, γ') experiments [6]) and observed in our spectra. Moore's 7.071 MeV level is probably the same one that we observe at 7.08 MeV. Because of this uncertainty in level identification we were unable to deduce a branching ratio for either of the 7 MeV states, and we feel that the value listed by Cramer *et al.* [12]), which relies upon such a level identification, may be incorrect.

4.2. ^{207}Pb

The coincidence spectra for ^{207}Pb are presented in fig. 9 along with the photon scattering cross section measured by Laszewski and Axel [1]). Peaks in $\sigma_{\gamma\gamma}$ occur at 4.8, 5.5, and 5.7 MeV, but some of the yield at 5.5 MeV can be attributed to ^{208}Pb in the target. We observe peaks near these same energies as well as at several others. In table 4 are listed the relative yields of the major peaks at bombarding energies corresponding to the analogs in ^{208}Bi of the $d_{5/2}p_{1/2}^{-1}$, $s_{1/2}p_{1/2}^{-1}$ and $d_{3/2}p_{1/2}^{-1}$ configurations in ^{208}Pb. The yields were computed by summing proton events in the peaks in coincidence with γ_0. The constant window width slightly enhances the yields of the lower energy states over what they would be if a constant γ-ray efficiency had been

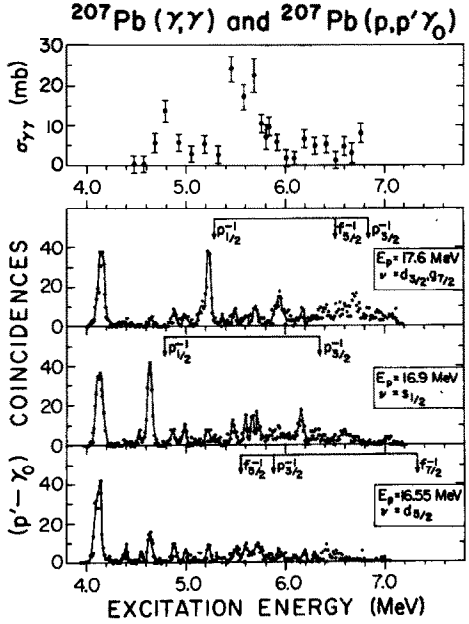

Fig. 9. $\sigma_{\gamma\gamma}$ [from ref. [1])] and (p, p'γ_0) coincidence spectra (present work) for ^{207}Pb. Window in γ-ray energy is $E_\gamma = E_{\gamma_0} \pm 500$ keV. Arrows indicate energies of particle-hole excitations relative to ^{207}Pb(g.s.) (see text and caption to fig. 7).

TABLE 4

Levels observed in ^{207}Pb(p, p'γ_0) and their relative yields on resonance

Energy (MeV)	Relative yield on resonance			Ref. [6]), (γ, γ)		Ref. [7]), (γ, γ)		Ref. [29]), (d, p)	
	$d_{5/2}$	$s_{1/2}$	$d_{3/2}$	energy	$g\Gamma_0^2/\Gamma$(eV)	energy	J^π	energy	J^π
4.10 / 4.14	156	151	145			4.104 4.140	$\frac{3}{2}^-$ $\frac{5}{2}^-$		
4.39	17	5	6					4.389	$\frac{5}{2}^+$
4.63	43	100	9			4.627		4.627	$\frac{1}{2}^+$
4.87	24	20	18	4.847 / 4.875	13	4.872	$\frac{1}{2}, \frac{3}{2}$	4.846 4.871	$\frac{5}{2}^+, \frac{7}{2}^-, \frac{7}{2}^+$
4.98	13	18	17	4.980	7	4.892	$\frac{1}{2}, \frac{3}{2}$	4.985	$\frac{1}{2}^+$
5.22	18	20	96	5.223	8			5.219	$\frac{3}{2}^+$
5.5	18	29	20	5.490	12				
5.6	23	28	16	5.600	8				
5.7	28	41	27	5.716	3				
5.9	14	22	43						
6.15	10	41	19						

used, but the correction is not significant for our qualitative approach and it does not affect the relative yields of a particular state on the three resonances.

4.10–4.14 MeV. Swann [7]) has suggested that the $\frac{3}{2}^-$, $\frac{5}{2}^-$ doublet results from the weak coupling of a $p_{1/2}$ neutron hole to the 2^+ collective state at 4.08 MeV in ^{208}Pb. Although the partially unresolved states are prominent in our spectra, our experimental geometry is not suitable for studying E2γ-ray transitions, and we have not pursued the analysis of these states. However the radiation from this doublet is strongly peaked in the reaction plane as is that from the 2^+ state in ^{208}Pb.

4.38 MeV. This level is weak in the p-γ_0 coincidence spectra because it decays mainly via γ_2. The p-γ_2 coincidence yield for this peak shows a strong $d_{5/2}$ resonance which identifies it as the $\frac{5}{2}^+$ state reported by Moyer *et al.* [29]) at 4.389 MeV in the ^{206}Pb(d, p) reaction; they found a spectroscopic factor $S_{d,p} = 0.77$. A configuration $\nu_{d_{5/2}} \otimes ^{206}$Pb(g. s.) was assigned by Hering *et al.* [30]). This state is clearly not described by weak coupling to an excitation of the ^{208}Pb core since there are no $d_{5/2}$ neutron states near 4.4 MeV in that nucleus. It is interesting to note, however, that if one thinks of the excitation as the promotion of a neutron from a $p_{1/2}$ to $d_{5/2}$ orbital, then the corresponding transition of a neutron in ^{208}Pb would lie higher in excitation because of the pairing force between $p_{1/2}$ neutrons in the ground state. The main $d_{5/2}p_{1/2}^{-1}$ configurations in ^{208}Pb lie at 4.973 MeV (3^-) and 5.036 MeV (2^-) [refs. [19,27])], an average of 620 keV higher in excitation, in good agreement with a difference of 628 keV between the neutron separation energies of ^{208}Pb and ^{207}Pb.

We have measured an excitation function for the 4.39 MeV state in the reaction ^{207}Pb(p, p'γ_2)^{207}Pb(4.39) between 16.1 and 17.6 MeV and found it to resemble the energy dependence of the (p, p') cross section of the 5.036 MeV, 2^- state in ^{208}Pb

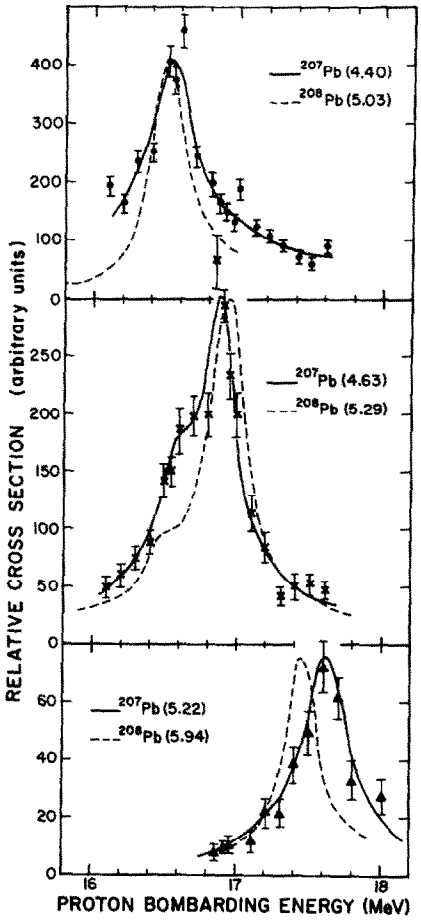

Fig. 10. Excitation functions over analog resonances for states in ^{208}Pb with dominant structure |particle $-p_{1/2}^{-1}\rangle\otimes$ ^{208}Pb(g.s.) [dashed curve is fit to data, fit and data from ref. [31])] and for states in ^{207}Pb with structure |particle $-p_{1/2}^{-2}\rangle\otimes$ ^{208}Pb(g.s.) (data and fits from present work).

measured by Wharton *et al.* [31]). Fig. 10 shows the two excitation functions normalized to the same peak cross section. It is the analog of the $d_{5/2}$ single-neutron state in ^{209}Pb which is responsible for the enhancement in ^{208}Pb(p, p') whereas the envelope of the ^{207}Pb(p, p'γ_2) cross section represents the combined analogs of all the $d_{5/2}p_{1/2}^{-1}$ fragments in ^{208}Pb. This fragmentation of the $d_{5/2}$ configuration strength in ^{208}Pb is probably responsible for the broadened resonance in ^{207}Pb(p, p').

4.63 MeV. The peak at 4.63 MeV is strongly enhanced on the $s_{1/2}$ analog resonance and is identified as the $\frac{1}{2}^+$ state seen in ^{206}Pb(d, p) to exhaust all of the spectroscopic strength of the configuration $\nu_{s_{1/2}}\otimes^{206}$Pb(g.s.) [ref. [29])]. The energy dependence of the (p, p'γ_0) cross section for this state and the (p, p') cross section for the 5.29 MeV 1^- state in ^{208}Pb [ref. [31])] are nearly identical, as can be seen from fig.

10b. No increase in the analog resonance width is observable in this case because of the extreme localization of the $s_{1/2}p_{1/2}^{-1}$ configuration in ^{208}Pb. The difference in excitation energies (5.29–4.63 MeV = 0.66 MeV) again reflects the breaking of a neutron pair in ^{208}Pb but not in ^{207}Pb. The 4.63 MeV state is therefore not representable by weak coupling of a $p_{1/2}$ hole to a ^{208}Pb core excitation.

In nuclear resonance fluorescence, Coope [6]) has noted the absence in ^{207}Pb of a doublet at 5.29 MeV which would be predicted by weak coupling to ^{208}Pb (5.29), but he does observe a group of levels at that energy in ^{209}Bi where a proton is coupled to the core. Similarly, we do not find in (p, p') the significant $s_{1/2}$ strength at 5.29 MeV which would be required in ^{207}Pb by the weak-coupling model. It is expected that the ^{209}Bi(p, p') reactions would selectively populate those levels near 17 MeV bombarding energy.

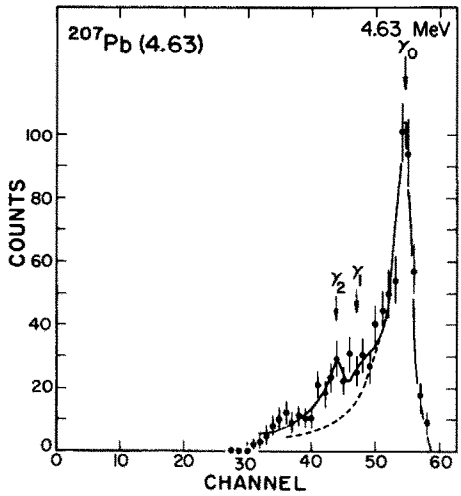

Fig. 11. Gamma-ray coincidence spectrum from the decay of ^{207}Pb (4.63). Dashed curve shows response function of NaI detector for γ_0 alone; solid curve is a least squares fit with three transitions allowed.

We have measured the γ-branching ratios of the 4.63 MeV level to the $\frac{1}{2}^-$ ground state and $\frac{3}{2}^-$ second excited states of ^{207}Pb. The γ-ray spectrum shown in fig. 11 has been fitted using the NaI response function obtained at 4.43 MeV from ^{12}C(p, p'γ). The γ-ray angular distributions are isotropic since the 4.63 MeV state has $J^\pi = \frac{1}{2}^+$. The singles proton yield was determined by bombarding on and off the $s_{1/2}$ resonance. Fig. 12 shows the proton spectra and the non-resonant background which was subtracted from the singles spectrum. We find $\Gamma_{\gamma_0}/\Gamma = 86 \pm 9\%$, $\Gamma_{\gamma_2}/\Gamma = 11 \pm 4\%$ and $\Gamma_{\gamma_1}/\Gamma \leq 3 \pm 6\%$, as listed in table 2. Since a pure $s_{1/2}p_{1/2}^{-2}$ configuration could not decay to a pure $p_{3/2}^{-1}$ hole state, the 11% γ_2 branch indicates that $p_{3/2}^{-1}$ amplitudes exist in the $\frac{1}{2}^+$ state.

4.87 and 4.98 MeV. Both of these peaks are about equally populated on the three IAR. The first corresponds closely in energy to the 4.84 MeV, 1^- state in ^{207}Pb and

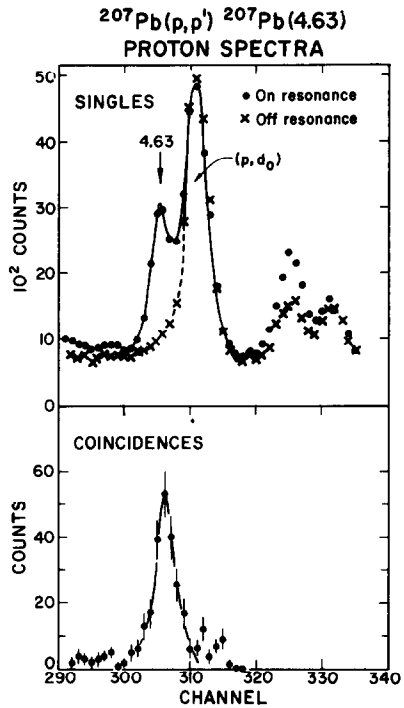

Fig. 12. Singles and coincidence particle spectra in vicinity of the 4.63 MeV $\frac{1}{2}^+$ state in ^{207}Pb. Singles spectra are shown both on and off the $s_{1/2}$ analog resonance. Dashed line through the off resonance data was used for background subtraction.

also to an enhancement in photon scattering in ^{207}Pb [ref. [1])]. Coope [6]) has reported a probable weak coupling doublet in ^{207}Pb at 4.847 and 4.875 MeV, levels which we would not have resolved. Fig. 13 compares our (p, p') excitation functions for the 4.84 MeV 1^- state in ^{208}Pb and the 4.87 MeV "state" in ^{207}Pb. Since both cross sections are apparently independent of energy, the argument for weak coupling is not compelling, but the data are nevertheless consistent with that picture. The 4.84 MeV level in ^{208}Pb is not populated by the (d, p) reaction [4,5]) so its $p^{-1}_{1/2}$ amplitude is small, an apparent requirement for the weak coupling model in these nuclei. We conclude that the weak coupling picture of the 4.847–4.875 MeV doublet is reasonable, but its proof must await determination of the spins and parities of the levels, and as seen in table 4 some confusion exists in that regard.

A state at 4.98 MeV has also been seen in (γ, γ) ref. [6])] and (d, p) [ref. [29])] reactions and assigned $J^\pi = \frac{1}{2}^+$. It is fairly weak in our spectra, and its resonance yield too featureless to assign it to a dominant configuration, especially in the absence of a corresponding state at the same excitation in ^{208}Pb.

5.22 MeV. This peak has a clear $d_{3/2}$ character and is again probably a single level, the $\frac{3}{2}^+$ state at 5.219 MeV excited strongly in the ^{206}Pb(d, p) reaction and found to

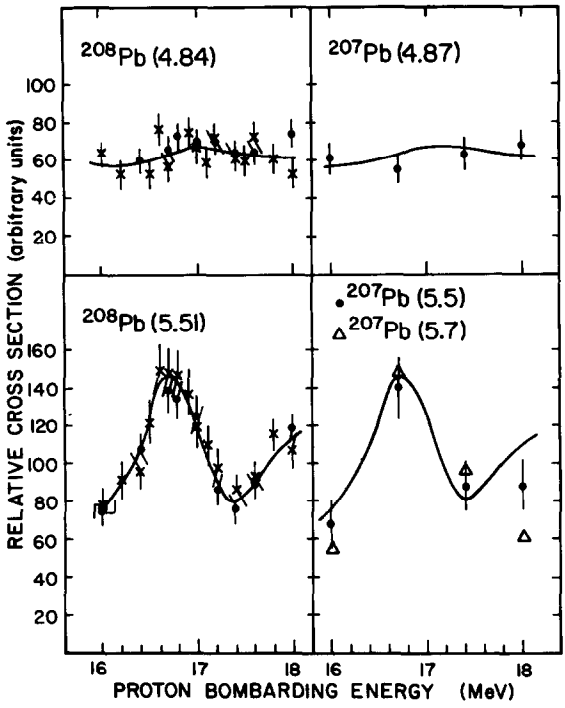

Fig. 13. Excitation functions for populating the 4.84 and 5.51 MeV states in ^{208}Pb and the 4.87, 5.5 and 5.7 MeV "states" in ^{207}Pb via (p, p'γ_0). Data points with solid circles were averaged over γ-ray angles, points with crosses are out of plane measurements only. Solid curve is drawn by eye through ^{208}Pb and reproduced for comparison with the ^{207}Pb data.

exhaust 53% of the $\nu_{d_{3/2}} \otimes ^{206}$Pb(g.s.) strength [25]). The (p, p') excitation function for this state is similar to that of the 5.94 MeV 1^- state in ^{208}Pb [31]) (see fig. 10c), which is predominantly $d_{3/2}p^{-1}_{1/2}$. The excitation energy difference, 0.72 MeV, is again reasonably close to the pairing energy.

5.5, 5.6 and 5.7 MeV. Our spectra show at least three peaks in this region rather poorly defined in energy, and there may be many levels contributing to the structures. Identification with levels seen in (γ, γ) experiments is speculative, but since it is the region of greatest dipole strength below threshold in ^{207}Pb [ref. [1])], weak coupling to ^{208}Pb(5.51) is an obvious possibility, particularly in light of the small $p^{-1}_{1/2}$ admixture in that state as shown by its absence in ^{207}Pb(d, p) [refs. [10,11])]. Excitation functions which we obtained for the 5.5 MeV groups in ^{207}Pb and ^{208}Pb are shown in fig. 13. The distinctive enhancement at 16.7 MeV bombarding energy seems to be present in both nuclei. The 5.7 MeV peak in ^{207}Pb shows this same behavior, though the second rise near 18 MeV does not occur. It seems clear, nevertheless, that the states near 5.5 and 5.7 MeV in ^{207}Pb have a structure that is closely related to that of the 5.51 MeV state in ^{208}Pb.

5.90 MeV. A peak with definite $d_{3/2}$ resonance character, but possibly consisting of many levels, is seen at about 5.9 MeV. Weak coupling to ^{208}Pb(5.94) is ruled out by the large $d_{3/2}/p_{1/2}^{-1}$ amplitude in that state.

6.15 MeV. This peak, showing an $s_{1/2}$ enhancement, has not been previously reported in particle or γ-ray experiments. Its excitation energy is close to that of the unperturbed shell-model configuration $s_{1/2}p_{3/2}^{-1}$ relative to ^{207}Pb(g.s.) , a structure which would limit its J^π to $\frac{1}{2}^+$, $\frac{3}{2}^+$, and/or $\frac{5}{2}^+$. A description in terms of $\nu_{p_{1/2}}^{-1} \otimes$ ^{208}Pb(6.31) weak coupling would rule out $\frac{5}{2}^+$. Such a coupling is a possibility since the 6.31 MeV 1^- state is predominantly $s_{1/2}p_{3/2}^{-1}$ with necessarily small $s_{1/2}p_{1/2}^{-1}$ admixtures, but the level is probably not collective in any sense. Additional support for the $s_{1/2}p_{3/2}^{-1}p_{1/2}^{-1}$ structure is provided by the existence of a strong peak with similar resonance behavior in our ^{206}Pb(p, p'γ_0) data, below. Moreover, in none of the Pb isotopes does the $s_{1/2}$ structure near 6 MeV have appreciable dipole strength in (γ, γ) experiments.

Above 6.15 MeV. No clearly defined peaks are seen, but a very broad distribution of $d_{3/2}$ strength extends between roughly 6.5 and 7 MeV.

To summarize the ^{207}Pb data, we clearly see the $\frac{5}{2}^+$, $\frac{1}{2}^+$, and $\frac{3}{2}^-$ single neutron states (relative to ^{206}Pb(g.s.)), and their resonance behavior parallels that of the analogous $\nu_{ip_{1/2}}^{-1}$ p-h parent states in ^{208}Pb. Weak coupling of a $p_{1/2}$ neutron hole to the 5.29 MeV ahd 5.94 MeV 1^- states in ^{208}Pb is prevented by the strong pairing interaction of the $p_{1/2}$ neutrons. Our data provide additional evidence for weak coupling of the 4.84 MeV and 5.51 MeV 1^- excitation to $p_{1/2}$ holes in ^{207}Pb. We also have some indications for $p_{1/2}^{-1}$ coupling to the 6.31 MeV 1^- state.

4.3. ^{206}Pb

The photon scattering work of Laszewski and Axel [1]) indicates that the inelastic scattering to the first 2^+ state in ^{206}Pb (at 0.831 MeV) is small compared to the elastic scattering for the states excited in (γ, γ). We expect that most 1^- states excited in ^{206}Pb(p, p') will similarly branch to the ground state whereas 2^- or 3^- couplings of the same p-h configurations will feed the 2^+ state or higher lying levels.

The spectra of protons in coincidence with ground-state γ-rays, shown in fig. 14, are characterized by mostly broad structures evidently comprised of many levels. The peaks in the elastic γ-ray scattering cross sections $\sigma_{\gamma\gamma}$ must also be the average contribution of many levels, since the strength observed in nuclear resonance fluorescence in ^{206}Pb is much less than in ^{208}Pb [ref. [3])], in contrast to the rather similar integrated cross sections measured with broad beam resolution [1]).

Perhaps the most obvious feature of the p'-γ_0 spectra is the absence of counterparts to the prominent peaks in ^{207}Pb and ^{208}Pb which have strong selective enhancement on a single IAR. The explanation of course lies in the dominant (particle $-p_{1/2}^{-1}$) neutron configurations of those levels, configurations which would not be available in a nucleus with a pure $p_{1/2}^{-2}$ ground state.

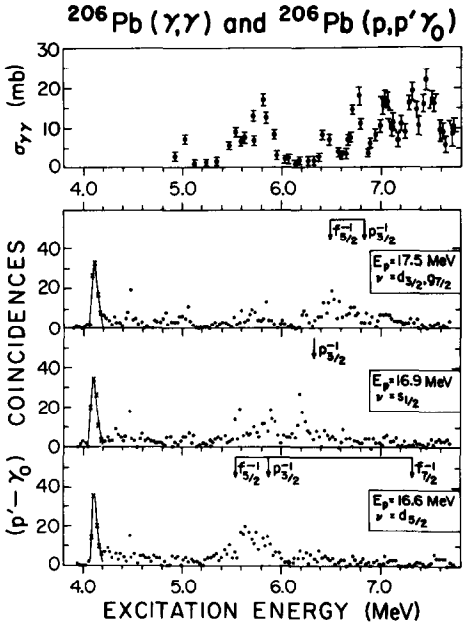

Fig. 14. $\sigma_{\gamma\gamma}$ [from ref. [1])] and (p, p'γ_0) coincidence spectra (present work) for ^{206}Pb. Window on γ-ray energy is $E_{\gamma_0} \pm 600$ keV.

Except for the 2^+ state at 4.1 MeV, we find no peaks which can be associated with levels known from resonance fluorescence experiments [6,7]). In ^{208}Pb most of the electric dipole strength below 6 MeV resides in the 5.51 MeV "collective" neutron particle-hole state. The γ-ray strength in ^{206}Pb is spread between 5.4 and 5.9 MeV, but it is still fairly concentrated and distinct from the 7 MeV "mini-resonance". We find an appreciable broad distribution of (p, p') strength in the 5.4–5.9 MeV region, enhanced at 16.6 and 16.9 MeV bombarding energy and weaker at 17.5 MeV. This energy dependence is reminiscent of the same excitation region in ^{207}Pb and ^{208}Pb. Although the E1 strength is spreading and shifting in energy as one moves from ^{208}Pb to ^{206}Pb, the shell-model structure of the envelope retains its integrity to a substantial degree.

A large peak in our $s_{1/2}$ spectrum at 6.2 MeV, not present in photoexcitation, falls close to the unperturbed energy of the $s_{1/2}p_{3/2}^{-1}$ shell model configuration. In ^{206}Pb the $p_{1/2}$ hole state is unavailable, so only $p_{3/2}^{-1}$ can couple with $s_{1/2}$ to give $J^\pi = 1^-$. The $s_{1/2}p_{3/2}^{-1}$ configuration resides mainly at 6.31 MeV in ^{208}Pb, and probably is responsible for the enhancement in the $s_{1/2}$ resonance of a peak in ^{207}Pb at 6.15 MeV. Thus despite the high level density of 1^- states at 6 MeV in ^{206}Pb, the $s_{1/2}p_{3/2}^{-1}$ configuration retains its location and localization in energy and persists as the dominant configuration in the vicinity. It is noteworthy that the $s_{1/2}p_{3/2}^{-1}$ configuration is only very weakly photoexcited in all three Pb isotopes.

Above 6.4 MeV, only $d_{3/2}$ strength is appreciable in our spectra. The structure in $\sigma_{\gamma\gamma}$ at about 6.5 MeV coincides in energy with a $d_{3/2}$ enhancement. Higher energy states are not significantly populated via (p, p') at these energies.

5. Conclusions

The (p, p'γ_0) reaction on Pb isotopes through isobaric analog resonances has been used to probe the p-h structure of states which have large ground-state γ-branches. The ground-state branches of four 1^- states in ^{208}Pb and a $\frac{1}{2}^+$ state in ^{207}Pb have been determined with 10% accuracy, and those of the 5.29, 5.94 and 6.31 MeV states in ^{208}Pb are found to be less than 100%. An 11% γ_2 branch of the 4.63 MeV $\frac{1}{2}^+$ state in ^{207}Pb is interpreted as an indication of $p_{3/2}^{-1}$ neutron amplitudes in that state. The non γ_0 decays of the ^{208}Pb levels unfortunately were not located in this experiment. Their identification in the future might shed more light on the structure of these 1^- levels.

Many of the states we observed in (p, p'γ_0) are the same as those seen in (γ, γ) experiments[1,6]). The (γ, γ) dipole strength distribution is surprisingly unaltered in its general features throughout the Pb isotopes. In contrast, the distribution of configuration strength revealed in (p, p') appears at first to be totally different in each isotope. However, many of these differences can be qualitatively explained by the coupling of valence $p_{1/2}$ neutron holes to 1^- excitations of the ^{208}Pb core.

Weak coupling of $p_{1/2}$ neutron holes in ^{207}Pb does not occur for core excitations with large $p_{1/2}$ hole amplitudes. Levels corresponding to neutron particle $p_{1/2}^{-1}$ excitations in ^{207}Pb are found with a nearly constant shift in excitation energy relative to analogous states in ^{208}Pb. The shift can be explained as a manifestation of the pairing interaction. The analog resonance excitation functions for particle $p_{1/2}^{-1}$ states in ^{208}Pb and ^{207}Pb are similar. As expected, particle $p_{1/2}^{-1}$ excitations are absent in ^{206}Pb.

When the $p_{1/2}^{-1}$ amplitude is known to be small in ^{208}Pb core excitations weak coupling of a $p_{1/2}$ hole becomes possible. Our data are consistent with the suggestion[6,7]) of weak coupling to the lowest 1^- state in ^{208}Pb. The 5.5 MeV "mini-resonance" retains its mixed p-h structure, but the energy shifts from 5.5 to 5.7 to 5.9 MeV as one moves from ^{208}Pb to ^{206}Pb. This argues against a strict weak coupling picture for the bulk of the dipole strength distribution. The $s_{1/2}p_{3/2}^{-1}$ configuration, not seen in photo-excitation, remains localized and constant in energy within 150 keV in the three isotopes studied, and must be viewed as essentially a ^{208}Pb core excitation even though the coupling of $p_{1/2}$ holes may not be strictly weak. At 6.2 MeV in ^{206}Pb, this excitation is the highest in energy whose parentage we can trace to ^{208}Pb. The peaks seen in γ-ray scattering at higher energies in ^{206}Pb are weakly excited by (p, p') and their relationship to dipole states near the same energies ^{208}Pb is not known.

Appendix

GAMMA-RAY ANGULAR CORRELATIONS

The directional correlation between protons and γ-rays in a (p, p'γ) reaction leading to a spinless final state can be expressed [32]) as

$$W_J(\theta, \phi) \propto \sum_{\sigma} \left| \sum_{m} (-1)^m P_m^J \, \mathrm{e}^{-\mathrm{i}m\phi} d_{m\sigma}^J(\theta) \right|^2 , \tag{A.1}$$

where J is the spin of the excited state of the residual nucleus, m is the z component of J, σ represents the γ-ray polarization, P_m^J is the population amplitude for the mth substate, and $d_{m\sigma}^J$ is a rotation matrix element. The polar and azimuthal angles θ and ϕ are defined by the coordinate system of fig. 15, whose quantization axis lies perpendicular to the reaction plane. In this coordinate system, the Bohr theorem [33]) requires that

$$\pi_\mathrm{i} \, \mathrm{e}^{\mathrm{i}\pi S_\mathrm{i}} = \pi_\mathrm{f} \mathrm{e}^{\mathrm{i}\pi S_f} \tag{A.2}$$

in which $\pi_\mathrm{i}(\pi_\mathrm{f})$ is the parity of the initial (final) nucleus and S is the sum of the spin components along z. The magnetic substates populated in spin-flip and non-spin-flip reactions are restricted by eq. (A.2) to the following possibilities for $J = 1^+$ and 1^- states.

$$\begin{array}{lll} & J_\mathrm{i}^\pi = 1^+ , & J_\mathrm{i}^\pi = 1^- , \\ \text{spin flip} & m = \pm 1 , & m = 0 , \\ \text{non flip} & m = 0 , & m = \pm 1 . \end{array}$$

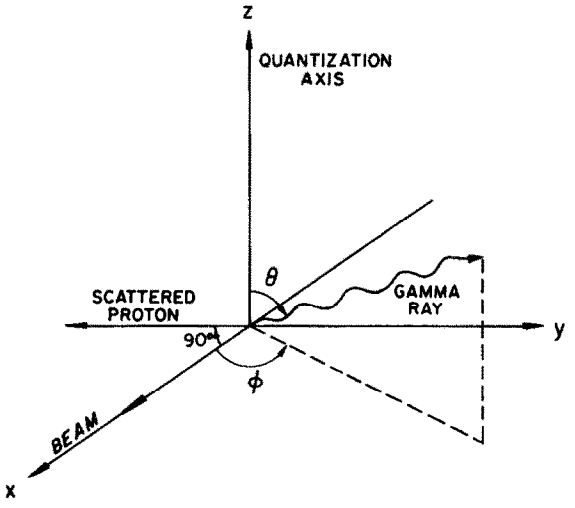

Fig. 15. Coordinate system used in the calculation of (p, p'γ) angular correlations.

Since spin-flip and non-flip amplitudes are incoherent, the correlation for $J = 1$ now becomes

$$W_1(\theta, \phi) \propto \sum_{\sigma} \left[|P_0^1 d_{0\sigma}^1(\theta)|^2 + \left| \sum_{m=\pm 1} p_m^1 \, e^{-im\phi} \, d_{m\sigma}^1(\theta) \right|^2 \right]. \tag{A.3}$$

The $d_{m\sigma}^J$ functions for $J = 1$ are:

$$d_{1\pm 1}^1(\theta) = \tfrac{1}{2}(1 \pm \cos\theta),$$

$$d_{0\pm 1}^1(\theta) = \sqrt{\tfrac{1}{2}} \sin\theta,$$

$$d_{-1\pm 1}^1(\theta) = \tfrac{1}{2}(1 + \cos\theta).$$

If we now define the real amplitudes and phases of the substate populations according to

$$p_m^1 \equiv \alpha_m \, e^{i\delta m},$$

with

$$\sum_m |P_m^1|^2 = \sum_m (\alpha_m)^2 = 1 \tag{A.4}$$

and substitute into eq. (A.3), we obtain

$$W_1(\theta, \phi) \propto (\alpha_1^2 + \alpha_{-1}^2)(1 + \cos\theta) + 2\alpha_0^2 \sin^2\theta + \alpha_1 \alpha_{-1} \sin^2\theta \cos(\delta - 2\phi), \tag{A.5}$$

where $\delta = \delta_1 - \delta_{-1}$. In the plane (IP) and normal to the plane (OP) eq. (A.5) reduces to

$$W_{\mathrm{IP}}(\phi) \equiv W(\theta = 90°, \phi) = A[(1 + a_0^2) + 2a_1 a_{-1} \cos(\delta - 2\phi)], \tag{A.6}$$

$$W_{\mathrm{OP}}(\phi) \equiv W(\theta = 0°, \phi) = 2A(1 - a_0^2), \tag{A.7}$$

where we have introduced the proportionality constant A. The in plane correlation $W_{\mathrm{IP}}(\phi)$ has the property that its average value can be obtained by measuring at two angles 90° apart. Thus

$$\begin{aligned} W_{\mathrm{IP}}(\phi) + W_{\mathrm{IP}}(\phi + 90°) &= A[(1 + a_0^2) + 2a_1 a_{-1} \cos\delta - 2\phi) \\ &\quad + A[(1 + a_0^2) - 2a_1 a_{-1} \cos(\delta - 2\phi)] \\ &= 2A(1 + a_0^2) = 2\langle W_{\mathrm{IP}} \rangle, \end{aligned} \tag{A.8}$$

In which the average value of W_{IP} is defined as

$$\langle W_{\mathrm{IP}} \rangle \equiv \tfrac{1}{2} \int_0^{\pi} W_{\mathrm{IP}}(\phi) \sin\phi \, \mathrm{d}\phi = A(1 + a_0^2). \tag{A.9}$$

The average value of the correlation over 4π solid angle is computed by integration of eq. (A.5). The result is

$$\frac{1}{4\pi} \int_{\Omega} W(\theta, \phi) \, \mathrm{d}\Omega = \tfrac{4}{3} \mathrm{A}. \tag{A.10}$$

Solving the equation

$$\frac{\langle W_{IP}\rangle}{W_{OP}} = \frac{1+a_0^2}{1-a_0^2}, \tag{A.11}$$

for a_0^2 and substituting into eq. (A.8), one obtains

$$A = \frac{2\langle W_{IP}\rangle + W_{OP}}{4}. \tag{A.12}$$

Using eq. (A.8) and putting the value of A into eq. (A.10) we have for the average of the correlation over all angles

$$\frac{1}{4\pi}\int_{\Omega} W(\theta,\phi)\,d\Omega = \tfrac{1}{3}[W_{IP}(\phi) + W_{IP}(\phi+90°) + W_{OP}]. \tag{A.13}$$

Thus the total γ-ray yield can be computed from measurements at three angles, two in the plane 90° apart and one normal to the plane.

References

1) R.M. Laszewski, Ph.D. thesis, University of Illinois, 1975 (unpublished); R.M. Laszewski and P. Axel, Phys. Rev. **C19** (1979) 342
2) A. de Shalit, Phys. Rev. **122** (1961) 1530
3) I. Hamamoto, Nucl. Phys. **A126** (1969) 545
4) G. Francillon, Y. Terrien and G. Vallois, Phys. Lett. **33B** (1970) 216
5) J.P. Coffin, N. Stein, T.P. Cleary, C.H. King and D.A. Bromley, Nucl. Phys. **A181** (1972) 337
6) D.F. Coope, L.E. Cannell and M.K. Brussel, Phys. Rev. **C15** (1977) 1977
7) C.P. Swann, Proc. Int. Conf. on photonuclear reactions and applications (US AEC Office of Information Services, Oak Ridge, Tennessee, 1973) p. 317
8) C.P. Swann, Nucl. Phys. **A201** (1973) 534
9) T.P. Cleary, N. Stein and P.R. Maurenzig, Nucl. Phys. **A232** (1974) 287
10) J. Bardwick and R. Tickle, Phys. Rev. **161** (1967) 1217
11) M. Dost and W.R. Hering, Phys. Lett. **26B** (1968) 443
12) J.G. Cramer, P. von Brentano, G.W. Phillips, H. Ejiri, S.M. Ferguson and W.J. Braithwaite, Phys. Rev. Lett. **21** (1968) 297
13) J.W. Knowles and A.M. Kahn, Bull. Am. Phys. Soc. **12** (1967) 583
14) T. Chapuran, R. Vodhanel and M.K. Brussel, Phys. Rev. **C22** (1980) 1420
15) W. Knüpfer, R. Frey, A. Freibel, W. Mettner, D. Meuer, A. Richter, E. Spamer and O. Titze, Phys. Lett. **77B** (1978) 367
16) E.D. Earle, A.J. Ferguson, G. van Middelkoop, G.A. Bartholemew and I. Bergqvist, Phys. Lett. **32B** (1970) 471
17) W.W. True, C.W. Ma and W.T. Pinkston, Phys. Rev. **C3** (1971) 2421
18) M. Harvey and F.C. Khanna, Nucl. Phys. **A221** (1974) 77
19) C.F. Moore, J.G. Kulleck, P. von Brentano and F. Rickey, Phys. Rev. **164** (1967) 1559
20) S. Raman, Proc. Int. Symp. on neutron capture gamma ray spectroscopy (Brookhaven National Laboratory and SUNY, Stony Brook, 1978) p. 193
21) C.P. Swann, Phys. Rev. Lett. **32** (1974) 1449
22) R.M. DelVecchio, S.J. Freedman, G.T. Garvey and M.A. Oothoudt, Phys. Rev. **C13** (1976) 2089
23) C.P. Swann, Phys. Rev. **C16** (1977) 2426
24) S.J. Freedman, C.A. Gagliardi, G.T. Garvey, M.A. Oothoudt and B. Svetitsky, Phys. Rev. Lett. **37** (1976) 1606

25) D.J. Horen, F.P. Calaprice, D. Mueller and R.T. Kouzes, Oak Ridge National Laboratory Report ORNL-5306 (1977) 114
26) A.M. Nathan, R. Starr, R.M. Laszewski and P. Axel, Phys. Rev. Lett. **42** (1979) 221
27) W.T. Wagner, G.M. Crawley, G.R. Hammerstein and H. McManus, Phys. Rev. **C12** (1975) 757
28) R.E. Marrs, E.G. Adelberger, K.A. Snover and M.D. Cooper, Phys. Rev. Lett. **35** (1975) 202; R.E. Marrs, Ph.D. thesis, University of Washington (unpublished), 1975
29) R.A. Moyer, B.L. Cohen and R.C. Diehl, Phys. Rev. **C2** (1970) 1898
30) W.R. Hering, A.D. Achterath and M. Dost, Phys. Lett. **26B** (1968) 568
31) W.R. Wharton, P. von Brentano, W.K. Dawson and P. Richard, Phys. Rev. **176** (1968) 1424
32) J.G. Cramer and W.W. Eidson , Nucl. Phys. **55** (1964) 593
33) A. Bohr, Nucl. Phys. **10** (1959) 486